

Experimental Study on Drying Biomass with a Spherical Heat Carrier

Xinya Huang, Taikun Yin, Gang Li,* Xiaoran Ma,* Yalei Wang, Zilin Li, Liang Liu, and Xinxin Liu

Cite This: *ACS Omega* 2023, 8, 27482–27487

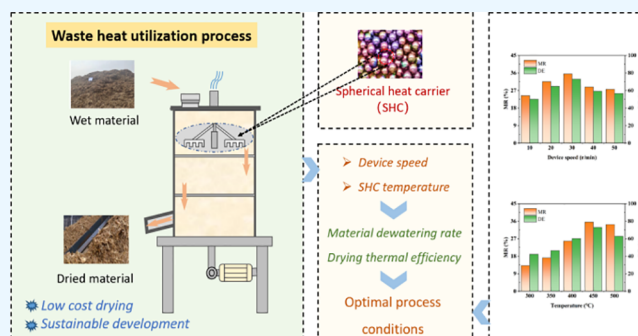
Read Online

ACCESS |

Metrics & More

Article Recommendations

ABSTRACT: Due to the reduction of the thermal efficiency and output fluctuation of the boiler system caused by the high moisture in biomass, dewatering of fuels using low-cost processes is an important step in feedstock pretreatment for biomass power plants. In the present study, a steel ball was used as the spherical heat carrier (SHC). The effects of the SHC temperature on the dewatering of different biomasses were investigated by a mixture-drying device at 40% moisture content of biomass, and the drying process of peanut shells was analyzed. Results showed that the moisture content was effectively reduced, and the combustion performance of the biomass was significantly promoted. The work is likely to provide an economically feasible approach for biomass drying in further studies.



1. INTRODUCTION

The development of renewable energy and the efficient utilization of traditional energy have become research hotspots because of energy scarcity and environmental pollution.¹ Typical renewable energy systems, such as solar, wind, and biomass, have the advantages of abundant resources, low carbon content, and being cheap. Unfortunately, the use of solar and wind energy is limited by the natural environment and is less stable.² Compared with solar and wind, biomass energy can be delivered over long distances without such concerns.³ Meanwhile, the supply and conversion facilities of biomass energy in China are satisfactory, by which the annual production of agricultural straw is about 939 Mt.⁴ It is implied that promoting the utilization of biomass energy is an inevitable choice for China facing energy challenges.

Currently, combustion for electricity generation is the most widespread and well-developed way to utilize biomass energy.^{5,6} The biomass power generation capacity has accounted for 70% of all generated renewable fuel power in Europe, and the installed capacity of biomass cogeneration is more than 12 GW in China.⁷ However, the high moisture content of biomass is a problem leading to material corruption in transit and increasing the boiler heat loss in the combustion of the material.⁸ In addition, it can aggravate the corrosion phenomenon and seriously affect the life of the boiler in operation.⁹ Bahadori¹⁰ and Li and Miao¹¹ found that the moisture content greatly influenced the thermochemical properties during direct combustion, and the thermal efficiency was inversely proportional to it. Therefore, drying (dewatering) is a necessary prior pretreatment step to the utilization of biomass materials.

Drying methods of biomass consist mainly of natural drying and artificial drying.¹² Low cost and simple operation are the obvious advantages of natural drying, but the industrial application is constrained by the large footprint, low drying efficiency, and unstable drying effect. Thus, the artificial drying method of forced dehydration by engineering becomes the basic method to ensure the stable operation. Microwave drying, hot air drying, and infrared drying are the common technologies.¹³ Yahya et al.¹⁴ used a solar-assisted fluidized bed to dry biomass. They found that the moisture content decreased from 20 to 14% in 1281 s, and the thermal efficiency of the system was 16.28% at a drying temperature of 78 °C. Amer et al.¹⁵ compared microwave drying with conventional oven drying. Results showed that microwave drying caused the surface of biomass to break down, and a drying rate of 30 times faster than that of conventional drying was provided. Lu et al.¹⁶ dried biomass bricks in a hot air environment with a temperature of 50 °C, a relative humidity of 32.1%, and a wind speed of 0.12 m/s. It was found that the moisture content and drying density decreased with the increase of drying time, which were 9.1% and 1.04 g/cm³, respectively, after 96 h. Chen et al.¹⁷ considered that radiation temperature was an important factor in the far-infrared drying process, and the overall drying time could be reduced by 59–

Received: May 3, 2023

Accepted: July 7, 2023

Published: July 21, 2023



66% as the radiation temperature increased from 100 to 200 °C. Obviously, artificial drying can effectively shorten the drying time and improve the drying efficiency. However, the existing technology has the disadvantages of high cost and low income because of high energy consumption. As a consequence, the low-cost and high-efficiency drying process becomes an urgent need in the market.

Biomass ash formed after the combustion of biomass is a complex mixture containing a large amount of organic matter, soil components, and other impurities.⁷ In 2019, the production of biomass ash from the power plants in China was nearly 500 Mt.¹⁸ A large amount of heat is taken away with the discharge of ash in the thermal power generation; thus, recycling waste heat from ash is quite a reasonable way which can noticeably reduce energy costs and improve the energy efficiency.¹⁹ Luo et al.²⁰ discussed the feasibility of using ash waste heat to prepare hydrogen-rich gas by biomass gasification. The results showed that when the ash temperature was 1200 °C and the ash particle size was below 2 mm, the gas production rate and H₂ content reached the maximum with 1.28 Nm³/kg of ash and 46.54%, respectively. Duan et al.²¹ established the ash waste heat recovery system and the coal gasification model. It was found that the ash waste heat could be effectively recovered by the system with a recovery rate of 83.08%. Meanwhile, the yield of syngas was 6.64 kmol/min at the optimum temperature of 800 °C and S/C ratio of 1.5. Hu et al.²² investigated the effect of ash waste heat on the gasification characteristics of coal under different process conditions. Their discovery indicated that the efficiency of the gasification reaction was positively correlated with the ash temperature. Besides, syngas productivity and carbon conversion efficiency reached a maximum of 67.9 and 91.7%, respectively. All the research mentioned above demonstrated the feasibility of recycling waste heat from ash and providing good economic benefits. Unfortunately, gasification reactions are limited by the cost and conditions in actual production.²³ Comparatively, the use of waste heat for biomass drying is simpler and not limited by the temperature of the chemical reaction. Onsree and Tippayawong²⁴ studied the kinetics of flue gas waste heat drying of biomass and showed that flue gas waste heat has a good effect on biomass drying. Li et al.²⁵ used the waste heat from the flue gas to dry pine chips, and their results showed that it can effectively reduce the moisture content and has good economic benefits.

Based on the current research progress mentioned above, a waste heat recovery method (Figure 1a) which stored the heat of biomass ash by using a steel ball as the spherical heat carrier (SHC) was proposed in our previous study. It was found that the proposed method was efficiently able to recover heat from the ash, and the efficiency of recovery under the optimum conditions was 77.4%.²⁶ In the present work, we proposed a SHC drying technology, which used the SHC to perform mixed direct contact drying of biomass in a mixture-drying device, as shown in Figure 1b. The industrial waste heat was the heat source of this technology, with the advantage of low drying cost. Furthermore, compared with torrefaction, the stirring of the device has a crushing effect on the material, which allows the material to be directly placed in the device without pretreatment such as grinding,²⁷ and a high heat and mass transfer rate could be obtained because the material had been in a state of motion.²⁸ A series of experiments were carried out to explore the influence of different process parameters on the drying effect. This paper can provide a

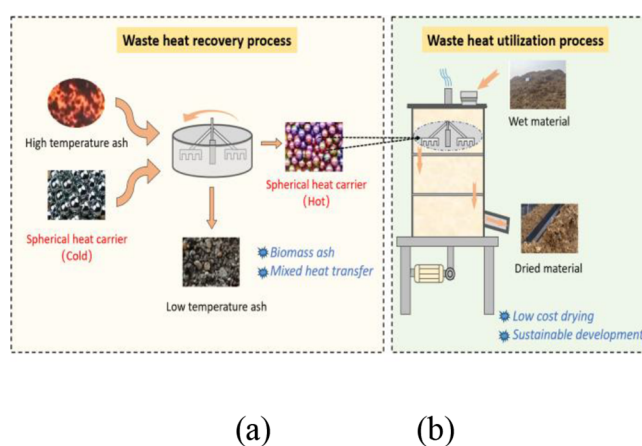


Figure 1. Recycling biomass ash waste heat (a) for drying high moisture biomass (b) process.

benchmark for the development and application of novel biomass drying processes.

2. EXPERIMENTAL SECTION

2.1. Experimental Materials. Peanut shells and straw were taken from the experimental fields of Henan Agricultural University, Zhengzhou, China, while woody debris were taken from Henan Hengguang Power Equipment Co., Ltd., China. The spherical heat carrier (SHC) was a solid steel ball with $D = 12$ mm (Henan Tianming Instrument and Equipment Co., Ltd., China).

2.2. Experimental Device. A stainless steel structure was used as the main body of the device, and aluminum silicate fibers were used to wrap the outer layer, as shown in Figure 2.

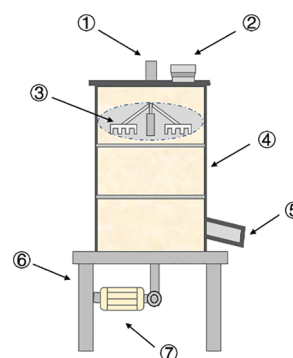


Figure 2. Mixture-drying device: (1) water vapor outlet; (2) material inlet; (3) stirrer; (4) cavity; (5) material outlet; (6) support; and (7) motor.

The whole device was divided into three layers with a height of 250 mm of each layer, and interlaced discharge ports were placed between the layers. The mixing speed of the material and SHC was regulated by a frequency conversion motor (CH/CV, Taiwan Yichuan Deceleration Motor Co., Ltd., China) with a maximum power of 750 W. In this work, the SHC with a high temperature and biomass materials with high moisture entered from the material inlet. They were rapidly mixed under the stirring of the stirring plate and gradually fell to the final layer. The water vapor produced during the drying process was brought out by the ventilating fan at the air outlet. As the temperature dropped to 30 °C, the SHC and dried materials were discharged from the material outlet. The K-type

thermocouple (Shenzhen Topper Electronics Co., Ltd., China) was used for measuring the temperature of the mixture in real time.

The other main instruments include an intelligent muffle furnace (KL-SWCK6, Hebi Keli Measurement and Control Technology Co., Ltd., China), an electric blast drying oven (DHG-942, Shanghai Yiheng Scientific Instruments Co., Ltd., China), an electronic balance (WT-N, Changzhou Wantai Balance Instrument Co., Ltd., China), and a temperature inspection instrument (TP700, Shenzhen Topper Electronics Co., Ltd., China).

2.3. Methods. The experiments were scheduled as follows: (1) Water was added to make the overall moisture content of the material reach 40% after the biomass was fully dried at 105 °C.²⁹ Then, it takes 24 h to make water evenly distributed. (2) The SHC was heated to the set temperature in the muffle furnace. After the temperature was held constant for 10 min, the SHC was taken out and mixed with biomass. (3) At a mass ratio of 2:1, the SHC with a mass of m_1 and the high moisture biomass with a mass of m_2 were mixed and placed into the device. Then, the agitator started to exchange heat rapidly. After the temperature of the mixture was reduced to 30 °C, the outlet was opened to take out the mixture, and the whole mixture was weighed as m_3 . The corresponding material dewatering rate (MR) and drying thermal efficiency (DE) were calculated with eq 1³⁰ and eq 2.³¹ (4) Industrial analysis was used to calculate the moisture, ash, volatiles, and fixed carbon content of the peanut shells in the SHC drying process. A field emission scanning electron microscopy system (Sirion 200, FEI, USA) was used to observe the morphology and microstructure of the material at a voltage of 5 kV and a resolution of 3.0 mm.

$$MR = \frac{m_1 + m_2 - m_3}{m_2 M_t} \times 100\% \quad (1)$$

$$DE = \frac{(m_1 + m_2 - m_3)\Delta H + (m_1 + m_2 - m_3)C_w(T_1 - T_2)}{C_i m_1 T_0} \times 100\% \quad (2)$$

where M_t is the initial moisture content of biomass (%), ΔH is the latent heat of vaporization of water (2257 kJ kg⁻¹), and C_i is the specific heat capacity of SHC, as shown in Table 1, C_w is

Table 1. Specific Heat Capacity of SHC at Different Temperatures

temperature (°C)	300	350	400	450	500
specific heat capacity (J g ⁻¹ °C ⁻¹)	0.54	0.55	0.56	0.565	0.57

the specific heat capacity of water (4.2 J g⁻¹ °C⁻¹), T_0 is the initial temperature of SHC (°C), T_1 is the boiling point of water (100 °C), and T_2 is the final temperature of the mixture (30 °C). It should be noticed that the total mass reduction was considered as the total moisture weight loss in the computational process.

3. RESULTS AND DISCUSSION

3.1. Effects of SHC Temperature on the Desiccation of Different Types of Biomasses. **3.1.1. Effect of SHC Temperature on the Desiccation of Straw.** Temperature gradient is an important driving force for heat and mass transfer, while high temperature may aggravate more heat loss. The effects of the SHC temperature on the drying effect of

straw under identical conditions of the device speed (30 r/min) and mass ratio (2:1) are depicted in Figure 3.

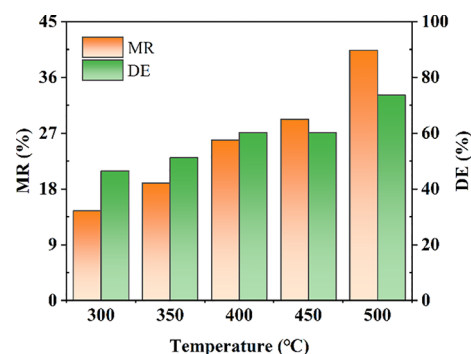


Figure 3. Effects of SHC temperature on the MR and DE of straw.

It can be seen that when the temperature of SHC was in the range of 300–450 °C, the DE was gradually increased with the increase of SHC temperature and then approached equilibrium, reaching a peak of 59.22% at 400 °C. Although the MR and DE were still increased at the temperature of 500 °C, it was found that a large amount of flue gas, the phenomenon of straw carbonization, and a heavy burnt taste were produced after the mixing of SHC and straw. The decomposition of cellulose, hemicellulose, and lignin above 220 °C caused higher theoretical values of MR and DE.³² Consequently, the optimum temperature of SHC for straw under this process was 400 °C, and the MR was 25.87%.

3.1.2. Effects of SHC Temperature on the Desiccation of Woody Debris. As shown in Figure 4, woody debris was used

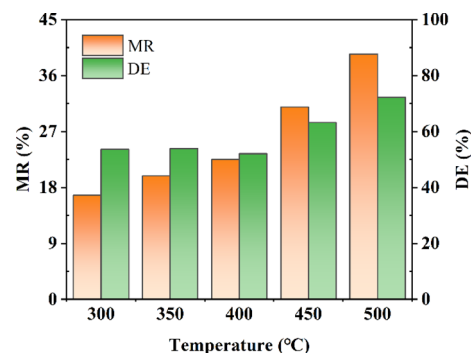


Figure 4. Effects of SHC temperature on the MR and DE of woody debris.

as the experimental material being dried, and the effects of the temperature of SHC on desiccation under an identical device speed of 30 r/min and mass ratio of 2:1 were investigated.

It was demonstrated that the MR clearly increased and DE fluctuated with the increase of the SHC temperature. The variation was likely caused by the fact that some lignin was softened at the SHC temperature of 350 °C, leading to a phenomenon of massive bonding by virtue of high temperature, which made the thermal conductivity of the woody debris worse, and the DE changed little, and even decreased at 350–400 °C.³² As the temperature of SHC increased above 400 °C, a similar phenomenon was observed in the desiccation experiments on straw, and a higher theoretical value of MR and DE was caused by the precipitation of volatiles. Therefore, no more than 350 °C of SHC temperature is a smart choice for

dry woody debris. Correspondingly, the MR and DE were 19.86 and 53.01%.

3.1.3. Effect of SHC Temperature on the Desiccation of Peanut Shells. The effects of the SHC temperature on the drying effect of peanut shells under identical conditions of device speed (30 r/min) and mass ratio (2:1) are depicted in Figure 5.

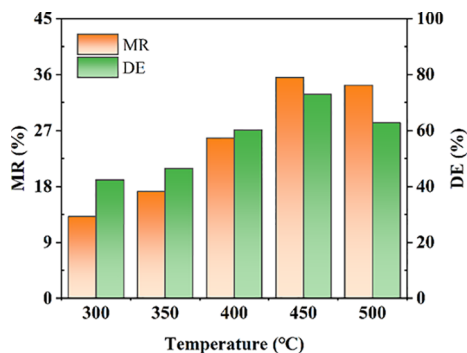


Figure 5. Effects of SHC temperature on the MR and DE of peanut shells.

It can be seen that the MR and DE first increased and then decreased as the temperature of SHC increased. In the SHC temperature range of 300–350 °C, the heating of the material itself was slow, and the MR and DE were relatively low. The highest MR and DE were 35.57 and 71.74%, respectively, at the SHC temperature of 450 °C, which then decreased over 500 °C because of the heat loss. Thus, the optimum SHC temperature for peanut shells under this process was 450 °C.

3.1.4. Analysis of the Energy Consumption. The specific energy consumption (SEC) of biomass under optimum conditions was compared. The calculation formula was described by eq 3³³

$$\text{SEC} = \frac{C_p m_1 T_0 + Pt}{m_1 + m_2 - m_3} \times 100\% \quad (3)$$

where P is the motor power, and t is the drying time. It was considered that the temperature of the SHC and material was consistent at the end of drying.

The calculation results showed that the SEC values of straw, woody debris, and peanut shells were 2.62 kW h/kg of water, 3.88 kW h/kg of water, and 1.81 kW h/kg of water, respectively. The SEC of microwave drying is between 3.38 and 6.90 kW h/kg of water, and the SEC of solar drying is between 3.23 and 8.80 kW h/kg of water.^{34,35} The SEC of the drying technology proposed in our study is not higher than that of microwave drying and solar drying. The heat used in this technology comes from the waste heat of ash, and the remaining energy consumption comes from the electrical energy of the device. Thus, our research has the advantage of low cost and provides an effective solution for the utilization of ash waste heat. Clearly, the SEC of peanut shells under the optimum conditions of this process was the lowest. Therefore, peanut shells were selected as the analysis object of our process.

3.2. Industrial Analysis. When the mass ratio of SHC to biomass was 2:1, the temperature of SHC was 450 °C, and the speed of the device was 30 r/min. The results of industrial analysis on peanut shells are shown in Table 2.

Table 2. Industrial Analysis Results of Peanut Shells

component	moisture (%)	ash (%)	volatile (%)	fixed carbon (%)
before drying	40.000	2.578	45.173	12.249
after drying	30.323	2.339	51.444	15.894

According to the results shown in Table 2, the moisture and ash content of dried peanut shells decreased by 24.19 and 9.27%, respectively, while the volatile and fixed carbon content increased to 13.9 and 29.8%, respectively. The decrease of moisture could not only ease the phenomenon of slag-buildup during combustion but also reduce the heat required for the evaporation of water during subsequent combustion.³⁶ The combustible components of biomass mainly exist in the form of flammable organic substances composed of carbon and hydrogen. The ash content is negatively correlated with the content of carbon and hydrogen, and the ash is generally presented in the form of SiO_2 , CaCO_3 , and some alkali metal salts and oxides. A large number of studies have shown that SiO_2 or silicon-containing substances have inhibitory effects on the gasification reaction rate of biomass.³⁷ Therefore, the reduction of ash could not only increase the content of combustible elements in the biomass fuels but also be beneficial for subsequent combustion, pyrolysis, gasification, and so forth. The heating value of the fuel will increase with the increase of volatiles and fixed carbon content.³⁸ The above analysis indicates that the appropriate process of SHC drying has a good effect on the combustion performance of peanut shells.

3.3. Analysis of SEM Characterization Results. The SEM results of the peanut shells under the mass ratio of 2:1, SHC temperature of 450 °C, and device speed of 30 r/min are displayed in Figure 6.

The results clearly showed that the surface of the peanut shells without desiccation was scaly, and the overall structure

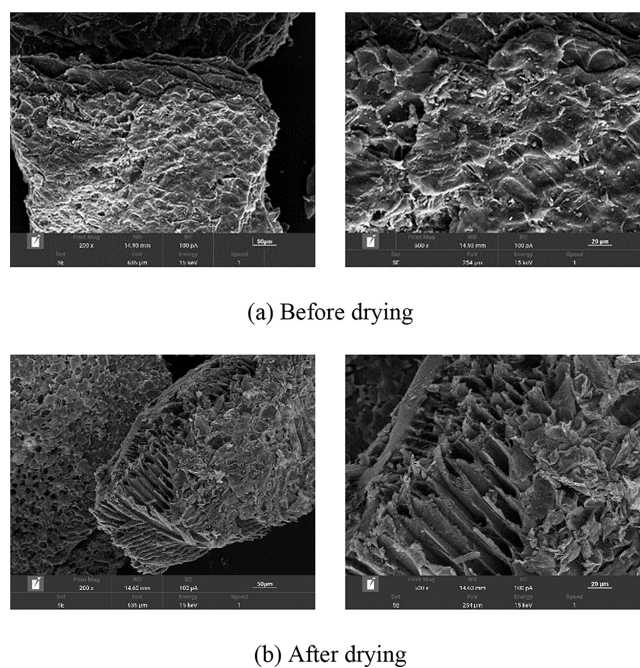


Figure 6. SEM image of the peanut shell surface before (a) and after (b) drying by SHC. The left was amplified by 200 times, and the right was amplified by 500 times.

was tight. However, due to the stirring effect of the device and the collision of SHC, the surface of the peanut shells was partially broken after desiccation. Compared to extraction, the internal pore channels of peanut shells were exposed, increasing the contact area between the peanut shell fuel and oxygen during subsequent combustion.³⁹ For biomass with poor thermal conductivity like peanut shells, the rough surface could not only increase the mass transfer in the combustion process but also facilitate the liberation of volatiles.¹⁵

3.4. Effects of the Device Speed on Desiccation. It was demonstrated that stirring the mixture material could effectively avoid the local overheating of materials, and the contact frequency between the material and the surface of SHC was affected by the rotation speed of the device.⁴⁰ We performed a large number of experiments to detect the effects of the device speed on the MR and DE of peanut shells under an identical SHC temperature of 450 °C and mass ratio of 2:1.

The results, as illustrated in Figure 7, show that the desiccation effect using MR and DE as the indicators was

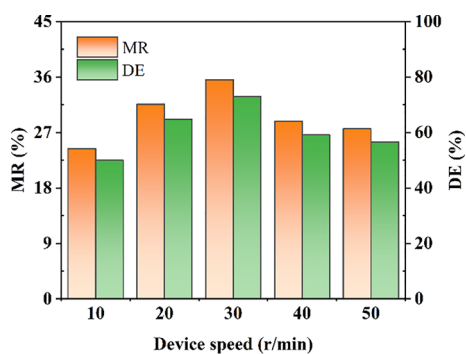


Figure 7. Effects of the device speed on the desiccation of peanut shells.

significantly influenced by the speed of the device. When the device speed was less than 30 r/min, the MR and DE increased with the increase of the device speed, and the peak values were 35.57 and 71.74%, respectively. When the device speed went beyond 30 r/min, the MR and DE showed a downward trend. This was attributed to the fact that the excessive rotation speed of the stirrer led to an increase of the gas flow rate in the device cavity on the one hand, which enhanced the heat transfer between air and SHC, and caused more heat loss. On the other hand, the collision frequency between the SHC and wall was increased, and the heat loss of SHC was aggravated.⁴¹ Therefore, the speed of the device was chosen to be 30 r/min.

4. CONCLUSIONS

It is an environmentally friendly way to dry the biomass using the waste heat from biomass power plants. It is possible to use the drying technology proposed in this paper, which effectively reduces the moisture content of the biomass and has a beneficial effect on subsequent combustion. In this paper, the effects of SHC temperature on the MR and DE were studied by experimental methods. The main conclusions were as follows. The SHC temperature plays a significant role in the dewatering process. The optimum SHC temperature for straw dewatering was 400 °C, corresponding to a MR of 25.87% and a DE of 59.22%. For woody debris, they were 350 °C, 19.86, and 53.01%, respectively, while for peanut shells, they were 450 °C, 35.57, and 71.74%, respectively. When the moisture

content was 40%, the mass ratio was 2:1, and the optimum speed of the drying device was 30 r/min.

AUTHOR INFORMATION

Corresponding Authors

Gang Li – College of Mechanical and Electrical Engineering, Henan Agricultural University, Zhengzhou 450002, China; Key Laboratory of New Materials and Facilities for Rural Renewable Energy, Ministry of Agriculture & Rural Affairs, Zhengzhou 450002, China; Email: ligang@henau.edu.cn

Xiaoran Ma – College of Mechanical and Electrical Engineering, Henan Agricultural University, Zhengzhou 450002, China; Key Laboratory of New Materials and Facilities for Rural Renewable Energy, Ministry of Agriculture & Rural Affairs, Zhengzhou 450002, China; Email: maxiaoran@henau.edu.cn

Authors

Xinya Huang – College of Mechanical and Electrical Engineering, Henan Agricultural University, Zhengzhou 450002, China; Key Laboratory of New Materials and Facilities for Rural Renewable Energy, Ministry of Agriculture & Rural Affairs, Zhengzhou 450002, China; orcid.org/0009-0004-7900-5003

Taikun Yin – College of Mechanical and Electrical Engineering, Henan Agricultural University, Zhengzhou 450002, China; Key Laboratory of New Materials and Facilities for Rural Renewable Energy, Ministry of Agriculture & Rural Affairs, Zhengzhou 450002, China

Yalei Wang – College of Mechanical and Electrical Engineering, Henan Agricultural University, Zhengzhou 450002, China; Key Laboratory of New Materials and Facilities for Rural Renewable Energy, Ministry of Agriculture & Rural Affairs, Zhengzhou 450002, China

Zilin Li – College of Mechanical and Electrical Engineering, Henan Agricultural University, Zhengzhou 450002, China; Key Laboratory of New Materials and Facilities for Rural Renewable Energy, Ministry of Agriculture & Rural Affairs, Zhengzhou 450002, China

Liang Liu – College of Mechanical and Electrical Engineering, Henan Agricultural University, Zhengzhou 450002, China; Key Laboratory of New Materials and Facilities for Rural Renewable Energy, Ministry of Agriculture & Rural Affairs, Zhengzhou 450002, China

Xinxin Liu – College of Mechanical and Electrical Engineering, Henan Agricultural University, Zhengzhou 450002, China; Key Laboratory of New Materials and Facilities for Rural Renewable Energy, Ministry of Agriculture & Rural Affairs, Zhengzhou 450002, China

Complete contact information is available at: <https://pubs.acs.org/10.1021/acsomega.3c03037>

Notes

The authors declare no competing financial interest.

ACKNOWLEDGMENTS

This work was supported by the Science and Technology Major Project of Henan Province (no. 221100110100), the Science and Technology Innovation Leader of Henan Province (no.234200510029), and the Science and Technology Project of Henan Province (no. 222102240099).

REFERENCES

- (1) Yu, J.; Jeon, C.-H. Virtual special issue of 2019 international symposium on clean energy and advanced carbon materials (CEAM-2019). *Energy Fuels* **2020**, *34*, 6521–6522.
- (2) Harrucksteiner, A.; Thakur, J.; Franke, K.; Sensfuß, F. A geospatial assessment of the techno-economic wind and solar potential of Mongolia. *Sustain. Energy Technol. Assess.* **2023**, *55*, No. 102889.
- (3) Akhtar, A.; Krepl, V.; Ivanova, T. A Combined overview of combustion, pyrolysis, and gasification of biomass. *Energy Fuels* **2018**, *32*, 7294–7318.
- (4) Cuiping, L.; Yanyongjie, Chuangzhi, W.; Haitao, H. Study on the distribution and quantity of biomass residues resource in China. *Biomass Bioenergy* **2004**, *27*, 111–117.
- (5) Zhao, M.; Han, Z.; Sheng, C.; Wu, H. Characterization of residual carbon in fly ashes from power plants firing biomass. *Energy Fuels* **2013**, *27*, 898–907.
- (6) Liu, Z.; Saydaliev, H. B.; Lan, J.; Ali, S.; Anser, M. K. Assessing the effectiveness of biomass energy in mitigating CO₂ emissions: Evidence from Top-10 biomass energy consumer countries. *Renew. Energy* **2022**, *191*, 842–851.
- (7) Wang, X.; Zhu, Y.; Hu, Z.; Zhang, L.; Yang, S.; Ruan, R.; Bai, S.; Tan, H. Characteristics of ash and slag from four biomass-fired power plants: Ash/slag ratio, unburned carbon, leaching of major and trace elements. *Energy Convers. Manage.* **2020**, *214*, No. 112897.
- (8) Han, J.; Choi, Y.; Kim, J. Development of the Process Model and Optimal Drying Conditions of Biomass Power Plants. *ACS Omega* **2020**, *5*, 2811–2818.
- (9) Yi, J.; Li, X.; He, J.; Duan, X. Drying efficiency and product quality of biomass drying: a review. *Dry. Technol.* **2020**, *38*, 2039–2054.
- (10) Bahadori, A.; Zahedi, G.; Zendejboudi, S.; Jamili, A. Estimation of the effect of biomass moisture content on the direct combustion of sugarcane bagasse in boilers. *Int. J. Sustain. Energy* **2014**, *33*, 349–356.
- (11) Li, Z.; Miao, Z. Effects of moisture and its input form on coal combustion process and NO_x transformation characteristics in lignite boiler. *Fuel* **2020**, *266*, No. 116970.
- (12) Desa, W. N. M.; Mohammad, M.; Fudholi, A. Review of drying technology of fig. *Trends Food Sci. Technol.* **2019**, *88*, 93–103.
- (13) Cong, X.-Y.; Miao, J.-K.; Zhang, H.-Z.; Sun, W.-H.; Xing, L.-H.; Sun, L.-R.; Zu, L.; Gao, Y.; Leng, K.-L. Effects of Drying Methods on the Content, Structural Isomers, and Composition of Astaxanthin in Antarctic Krill. *ACS Omega* **2019**, *4*, 17972–17980.
- (14) Yahya, M.; Fudholi, A.; Sopian, K. Energy and exergy analyses of solar-assisted fluidized bed drying integrated with biomass furnace. *Renew. Energy* **2017**, *105*, 22–29.
- (15) Amer, M.; Nour, M.; Ahmed, M.; Ookawara, S.; Nada, S.; Elwardany, A. The effect of microwave drying pretreatment on dry torrefaction of agricultural biomasses. *Bioresour. Technol.* **2019**, *286*, No. 121400.
- (16) Lu, Z.; Ma, C.; Zhao, Z.; Jia, W.; Wang, M. Effects of hot air drying time on properties of biomass brick. *Appl. Therm. Eng.* **2016**, *109*, 487–496.
- (17) Chen, N. N.; Chen, M. Q.; Fu, B. A.; Song, J. J. Far-infrared irradiation drying behavior of typical biomass briquettes. *Energy* **2017**, *121*, 726–738.
- (18) Zhao, B.; Xie, H.; Ren, C.; Liu, S.; Zhu, D.; Guan, H.; Wang, J. Application of biomass power plant ash as building materials. *Sci. Technol. Eng.* **2022**, *22*, 6802–6811. (In Chinese)
- (19) Gebreegziabher, T.; Oyedun, A. O.; Luk, H. T.; Lam, T. Y. G.; Zhang, Y.; Hui, C. W. Design and optimization of biomass power plant. *Chem. Eng. Res. Des.* **2014**, *92*, 1412–1427.
- (20) Luo, S.; Zhou, Y.; Yi, C. Hydrogen-rich gas production from biomass catalytic gasification using hot blast furnace slag as heat carrier and catalyst in moving-bed reactor. *Int. J. Hydrogen Energy* **2012**, *37*, 15081–15085.
- (21) Duan, W.; Yu, Q.; Wang, K.; Qin, Q.; Hou, L.; Yao, X.; Wu, T. ASPEN Plus simulation of coal integrated gasification combined blast furnace slag waste heat recovery system. *Energy Convers. Manage.* **2015**, *100*, 30–36.
- (22) Hu, Z.; Qu, A.; Zhong, Z.; Zhang, X.; Peng, H.; Li, J. Study on pulverized coal gasification using waste heat from high temperature blast furnace slag particles. *Int. J. Hydrogen Energy* **2021**, *46*, 26848–26860.
- (23) Matamba, T.; Iglauer, S.; Keshavarz, A. A progress insight of the formation of hydrogen rich syngas from coal gasification. *J. Energy Inst.* **2022**, *105*, 81–102.
- (24) Onsree, T.; Tippayawong, N. Analysis of reaction kinetics for torrefaction of pelletized agricultural biomass with dry flue gas. *Energy Rep.* **2020**, *6*, 61–65.
- (25) Li, H.; Chen, Q.; Zhang, X.; Finney, K. N.; Sharifi, V. N.; Swithenbank, J. Evaluation of a biomass drying process using waste heat from process industries: A case study. *Appl. Therm. Eng.* **2012**, *35*, 71–80.
- (26) Li, G.; Li, Z.; Yin, T.; Ren, J.; Wang, Y.; Jiao, Y.; He, C. Drying biomass using waste heat from biomass ash by means of heat carrier. *BioResources* **2022**, *17*, 5243–5254.
- (27) Trubetskaya, A.; Grams, J.; Leahy, J. J.; Johnson, R.; Gallagher, P.; Monaghan, R. F. D.; Kwapinska, M. The effect of particle size, temperature and residence time on the yields and reactivity of olive stones from torrefaction. *Renew. Energy* **2020**, *160*, 998–1011.
- (28) Qin, Y.; Lv, X.; Bai, C.; Qiu, G.; Chen, P. Waste heat recovery from blast furnace slag by chemical reactions. *JOM* **2012**, *64*, 997–1001. 893
- (29) O’Kelly, B. Oven-Drying characteristics of soils of different origins. *Dry. Technol.* **2005**, *23*, 1141–1149.
- (30) Zhang, N.; Shi, L.; Qi, H.; Xie, Y.; Cai, L. Effect of radio frequency (RF) drying technology on dehydration rate and energy consumption of Australia lignite. *Dry. Technol.* **2016**, *34*, 161–166.
- (31) Guo, J.; Zheng, L.; Li, Z. Microwave drying behavior, energy consumption, and mathematical modeling of sewage sludge in a novel pilot-scale microwave drying system. *Sci. Total Environ.* **2021**, *777*, No. 146109.
- (32) Yang, H.; Yan, R.; Chen, H.; Lee, D. H.; Zheng, C. Characteristics of hemicellulose, cellulose and lignin pyrolysis. *Fuel* **2007**, *86*, 1781–1788.
- (33) Motevali, A.; Minaei, S.; Banakar, A.; Ghobadian, B.; Khoshtaghaza, M. H. Comparison of energy parameters in various dryers. *Energy Convers. Manag.* **2014**, *87*, 711–725.
- (34) Kaveh, M.; Abbaspour-Gilandeh, Y.; Nowacka, M. Comparison of different drying techniques and their carbon emissions in green peas. *Chem. Eng. Process.* **2021**, *160*, No. 108274.
- (35) Yahya, M. Performance Analysis of Solar Assisted Fluidized Bed Dryer Integrated Biomass Furnace with and without Heat Pump for Drying of Paddy. *Int. J. Photoenergy* **2016**, *2016*, 1–17.
- (36) Qi, X.; Song, G.; Song, W.; Yang, S.; Lu, Q. Effects of wall temperature on slagging and ash deposition of Zhundong coal during circulating fluidized bed gasification. *Appl. Therm. Eng.* **2016**, *106*, 1127–1135.
- (37) Trubetskaya, A. Reactivity Effects of Inorganic Content in Biomass Gasification: A Review. *Energies* **2022**, *15*, No. 3137.
- (38) Kim, H.-J.; Oh, S.-C. Hydrothermal Carbonization of Spent Coffee Grounds. *Appl. Sci.* **2021**, *11*, No. 6542.
- (39) Trubetskaya, A.; Attard, T. M.; Budarin, V. L.; Hunt, A. J.; Arshadi, M.; Grams, J. Supercritical Extraction of Biomass-A Green and Sustainable Method to Control the Pyrolysis Product Distribution. *ACS Sustainable Chem. Eng.* **2021**, *9*, 5278–5287.
- (40) Kaveh, M.; Abbaspour-Gilandeh, Y. Impacts of hybrid (convective-infrared-rotary drum) drying on the quality attributes of green pea. *J. Food Process Eng.* **2020**, *43*, No. 13424.
- (41) Kaensup, W.; Chutima, S.; Wongwiset, S. Experimental study on drying of chilli in a combined microwave-vacuum-rotary drum dryer. *Dry. Technol.* **2002**, *20*, 2067–2079.